Simple synthesis route for fabrication of protective photo-crosslinked poly(zwitterionic) membranes for application in non-enzymatic glucose sensing

Adrian Olejnik[1,2*], Jakub Karczewski[3], Anna Dołęga[4], Katarzyna Siuzdak[1], Adam Cenian[1] and Katarzyna Grochowska[1]

[1]Centre for Plasma and Laser Engineering, The Szewalski Institute of Fluid-Flow Machinery, Polish Academy of Sciences, Fiszera 14 St., 80-231 Gdańsk, Poland

[2]Gdańsk University of Technology, Narutowicza 11/12 St., 80-233 Gdańsk, Poland

[3]Faculty of Applied Physics and Mathematics, Gdańsk University of Technology, Narutowicza 11/12 St., 80-233 Gdańsk, Poland

[4]Department of Inorganic Chemistry, Faculty of Chemistry, Gdańsk University of Technology, Narutowicza 11/12 St., 80-233 Gdańsk, Poland

*corresponding author e-mail: aolejnik@imp.gda.pl

Other e-mails in order:

jakub.karczewski@pg.edu.pl

anna.dolega@pg.edu.pl

ksiuzdak@imp.gda.pl

adam.cenian@imp.gda.pl

kgrochowska@imp.gda.pl

Data availability statement

Data available on request form the authors.

Funding statement

This work was supported by the National Centre for Research and Development via grant no LIDER/2/0003/L-8/16/NCBR/2017.

Conflict of interests disclosure

Authors declare no conflict of interests

Abstract

This work focuses on the fabrication of non-enzymatic glucose sensing material based on laser-formed Au nanoparticles embedded in Ti textured substrates. Those materials possess good catalytic activity

towards glucose oxidation in 0.1 X Phosphate Buffered Saline as well as resistance to some interferants such as ascorbic acid, urea, and glycine. Electrodes are further coated with three different polymers, i.e., Nafion, photo-crosslinked poly(zwitterions) based on sulfobetaine methacrylate and hybrid membrane consisting of both polymers. Both optimal integrity of the material and catalytic activity towards glucose oxidation were maintained by hybrid membranes with a large excess of poly(zwitterions) (mass ratio 20:1). Chemical structures of as-formed membranes are confirmed by Fourier Transform Infrared Spectroscopy. Due to the zwitterionic nature of coating, the electrodes are resistant to biofouling and maintain electrochemical activity towards glucose for 4 days. Moreover, due to the synergistic effect of both Nafion and poly(zwitterions), the interference from two compounds, namely from acetylsalicylic acid and acetaminophen, was diminished, i.e.. Besides the presence of polymer membranes, the electrode possesses a sensitivity of 36.8 $\mu A\ cm^{-2}\ mM^{-1}$ in the linear range of 0.4 – 12 mM, while the limit of detection was estimated to be 23 μM. Lastly, the electrodes are stable and their response is not altered even by 1000 bending cycles.

Keywords

Poly(zwitterions), glucose sensing, membranes, gold nanoparticles, PBS

Introduction

Considering the gradually increasing population of diabetics, there is an urgent need for fabrication of stable, inexpensive glucose sensing platforms. It is also especially important to develop technologies that allow noninvasive glucose sensing based on biofluids like sweat, saliva and tears [1]. The market is monopolized by electrochemical devices based on glucose-oxidase modified electrodes. However, their response is fragile to pH changes as well as can be seriously diminished when the temperature exceeds 40°C [2,3]. On the contrary, non-enzymatic glucose sensors have generally longer lifetime and higher stability than traditional enzymatic sensors, because they are devoid of biological components [4]. Typically, non-enzymatic sensing electrodes consist of metals such as Pt [5], Au [6], Pd [7], or metal/metal oxide Ni [8], Cu [9], Co [10] nanostructures. The mechanism of glucose detection is almost always based on direct electron transfer between glucose molecules and electrode surface [2,11]. For example, in the case of gold nanoparticles, it is well established that during anodic polarization $AuOH_{ads}$ species are formed which are capable of oxidizing glucose to gluconolactone [2]:

$$Au + OH^- \rightarrow AuOH_{(ads)} + e^-$$

$$Glucose_{(ads)} + 2AuOH_{(ads)} \rightarrow Gluconolactone + 2Au$$

Since the presence of hydroxyl ions is required for $AuOH_{ads}$ formation, the overall process is kinetically sluggish in neutral pH [2]. However, there are two crucial factors that prevent non-enzymatic glucose sensors from being commercially applicable: interference and biofouling. The first concept is related to the electrooxidation of various organic compounds other than glucose, e.g. aminoacids, ascorbic acid (AA), acetaminophen (AAp) [12], lactic acid (LA) [13] as well as acetylsalicylic acid (AsA) and urea [14]. They possess a particular property, namely, their molecules undergo oxidation at the same potential range as glucose along a similar mechanism. Therefore, the amperometric signals interfere and distort the results of glucose detection measurement. Negative effects connected with the presence of chlorides also fall into this category [2]. Those arguments confirm the necessity of characterizing glucose sensing materials in neutral pH environments containing physiological concentrations of chloride anions. The second concept, i.e., biofouling, is caused by the adsorption of different biomolecules such as proteins, lipids, or even whole cells onto the surface of the electroactive material. As-created biofilm diminishes or even entirely inhibits electron transfer and deteriorates the performance of the electrode [15].

One of the easiest methods of protecting the electrode from two negative factors described above is introducing various coatings or semi-permeable membranes, which prevent the access of biomolecules to the vicinity of the electrode [15]. Usually two types of polymers are incorporated in this method. One of them serves as a barrier for interfering compounds and the second one blocks proteins and provides biocompatibility. This strategy even had its first clinical applications, where a mixed Nafion/Kel-F/MPC (2-methacryloyloxyethyl phosphorylcholine) hybrid membrane was developed [3].

An important aspect of the last compound, MPC, was its zwitterionic structure, namely, its molecules possess one positively ($-R_4N^+$) and one negatively charged ($-RPO_3^-$) functional group. It is well established that this setup leads to a significant reduction of biomolecules' nonspecific adsorption [16,17]. The same effect can be achieved for polymeric zwitterions (PZ) [16,18]. Those macromolecules are typically based on, e.g., sulfobetaine methacrylate (pSBMA) or carboxybetaine methecrylate (pCBMA) derivatives. Due to intense dipol-dipol and dipol-counterion interactions, PZs are capable of both reducing entropy and increasing the enthalpy of protein adsorption, making this process thermodynamically unfavorable. Detailed description of the mechanisms that underlay this phenomenon was given by Schlenoff [16].

Photopolymerization is a facile method of obtaining various coatings which is frequently applied in different areas of science and industry such as photolithography [19] and corrosion protection [20]. The setup for photopolymerization consists of monomer, crosslinker, photoinitiator, UV light source, and stabilizers if needed. This process is based on the UV photon absorption by the photoinitiator and the subsequent creation of its excited states. During relaxation, free radicals are created on the monomers and crosslinker molecules. Then the polymerization goes according to the standard free radical mechanism. Depending on the power density of the light source and the formulation, one can change the reaction rates and crosslinking density and therefore the final mechanical and thermal properties of the membrane [21,22]. The majority of photopolymerized materials are crosslinked methacrylates and their derivatives [21,23]. The typical structure of such a coating consists of a large number of short interconnected chains [18]. Advantages of this method are relatively short time of exposure and small apparatus requirement. There is however one limitation of this technique, namely, it should be carried out under an atmosphere without oxygen. Oxygen can quench the excited states of the photoinitiator, as well as react with macroradicals. Both phenomena result in a serious decrease of the net molecular mass and therefore in altered properties of the coating [21]. It should be underlined that the photopolymerization method was also successfully applied to the synthesis of crosslinked poly(zwitterions) for glucose biosensors [24,25].

This work is a continuation of our previous research [14,26] connected to the application of Au nanoparticles (AuNP) based non-enzymatic glucose sensing platform covered with Nafion coating. Using a special electrochemical protocol we showed that Nafion does not provide a proper protection against interfering species due to blocking of the pores and adsorption on the metal | polymer interface. Also it does not provide the long-term stability in the presence of the human serum. Therefore, the purpose of this work is to propose an improvement of the typically used Nafion by combining it with poly(zwitterions) so that the selectivity of the material towards glucose sensing is increased in neutral media.

We present here a simple synthesis route for fabrication of protective photo-crosslinked poly(zwitterionic) membranes for application in non-enzymatic glucose sensing. The purpose of these membranes is the reduction of interference and biofouling. The chosen electrode material consists of titanium nanodimples, with embedded gold nanoparticles formed during 532 nm pulsed laser dewetting of a thin gold film. Similar substrates, although dewetted in a furnace, with Nafion membrane were introduced previously [26]. Then a mixture of zwitterionic monomers is cast onto the surface and photopolymerized in the presence of different amounts of crosslinking agent. Moreover, in addition to pure PZ, a hybrid coating consisting of both Nafion and poly(zwitterions) is introduced (Nafion – co – PZ). Metallic substrate morphology was confirmed using Scanning Electron Microscopy (SEM) and the functional group composition of the membrane was verified by Fourier Transform Infrared Spectroscopy (FT-IR). Electrochemical properties were tested by Cyclic Voltammetry (CV) and Electrochemical Impedance Spectroscopy (EIS).

In our previous research, to remain integrity, Nafion had to be heated at 120°C for a few minutes in order to retain adhesion after long-term immersion in the electrolyte. The advantage of hybrid (Nafion-co-PZ) coating is that it does not require this step in the sysntesis. Additionally time of the photopolymerization is relatively small (2 minutes after optimization). As a result of addition of polyzwitterion into the coating the long-term stability in diluted human serum was improved and for 10 days electrochemical signal was sustained.

Experimental

Reagents

Titanium foil (99.7%) was obtained from Strem and gold target (99.99 %) for magnetron sputtering from Quorum Technologies. Acetone, ethylene glycol, ammonium fluoride, glucose, lactic acid, glycine, and ascorbic acid were acquired from Chempur, while potassium ferrocyanate (II) and (III), urea, KCl and ethanol from POCH and Phosphate Buffered Saline (PBS) from Santa Cruz Biotechnology, respectively. Nafion resin solution (5% in water and lower aliphatic alcohols), acetaminophen, acetylsalicylic acid, glutamic acid, arginine and oxalic acid were bought from Sigma-Aldrich. Sulfobetaine methacrylate (SBMA), 2-Hydroxy-2-methylpropiophenone, ethylene glycol methacrylate (EGDMA) and Human serum (sterile-filtered from human male plasma AB, H4522) were also purchased from Sigma-Aldrich. Hydrolab HLP-5 system was used for deionization of water (0.05 μS).

Electroactive material preparation

Electroactive material was prepared along the route described thoroughly in our previous papers [26,27]. Briefly, the titanium foil was cut into 2×4 cm^2 pieces and sonicated with acetone, ethanol, and deionized water. Then, the plates were anodized at 40 V in an electrolyte containing 0.27 M NH_4F

dissolved in water/ethylene glycol solution (1/99). The electrochemical oxidation led to the formation of regular arrays of titania nanotubes. The subsequent exposure of TiO_2 nanotubes to oxalic acid caused etching of TiO_2 leaving a nanodimpled titanium topography (TiND). In order to obtain gold nanoparticles a 10 nm thin gold layer was magnetron sputtered onto TiND templates using Q150T S system (Quorum Technologies) with 13 nm/min rate in the presence of argon. Then, the plates were laser dewetted with a wavelength of 532 nm and fluence equal to 60 mJ/cm^2. Additionally, a motorized table was utilized to obtain well-defined patterns exposed to laser radiation.

Application of coatings

Three types of coatings were used for the purpose of the presented studies. First of them is poly(sulfobetaine methacrylate) crosslinked with ethylene glycol dimethacrylate. Those two reagents were mixed with different molar ratios (1:10, 1:100, and 1:1000). Water was added to the mixture so that the monomer concentration was equal to 5M. Then the crosslinking agent was added to solution (1 wt. %). As prepared, mixture was drop cast onto each plate with a density of 8 μL/cm^2. Electrodes with the applied polymerization mixture were immediately put into the photopolymerization chamber. The chamber consisted of a glass vessel equipped with quartz window, UV mercury lamp, and gas inlet and outlet ports. Plates were exposed to UV radiation for different times ranging from 1 to 100 minutes. The whole process was conducted under argon atmosphere.

Nafion coatings were obtained via drop casting of resin solution onto the surface of the electrode material and then thermal treatment at 120°C for 3 minutes. The deposition procedure was based on the previous reports [26,28].

Third, the hybrid coating consists of both pSBMA:EGDMA and Nafion. Three experimental strategies were examined: drop casting, Nafion and then photopolymerization according to the abovementioned procedure (Nafion | PZ), photopolymerization and then drop casting of Nafion (PZ | Nafion) and finally photopolymerization of SBMA:EGDMA mixture in the presence of Nafion (Nafion – co – PZ). Optimal Nafion : PZ mass ratio was equal to 1:20 and this type of coating is discussed the most thoroughly although information for other coatings is included in supporting information file in Fig. S2-S5. Some of the coatings had the tendency to swelling. Preliminary determination of swelling by naked eye allowed to exclude some of them. All types of membranes used in this work are schematically presented in Fig. 1

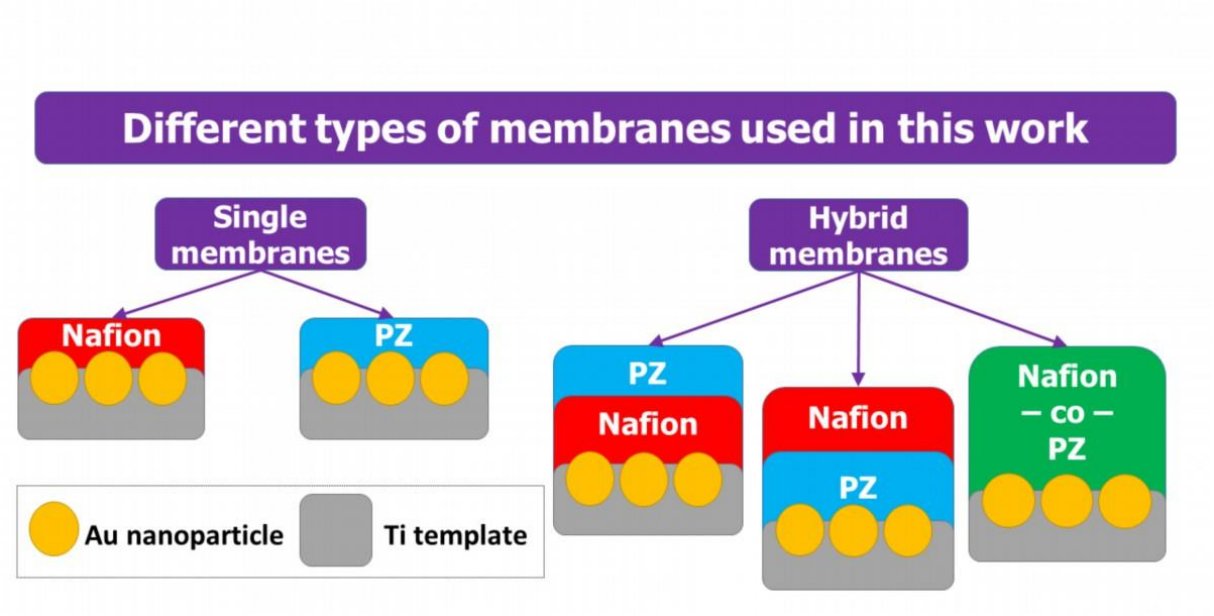

Fig. 1 A schematic diagram describing the different types of Nafion and poly(zwitterionic) membranes synthesized in this work.

Morphology and spectroscopic analysis

The morphology of the electrodes was investigated by means of the Schottky field emission scanning electron microscope (SEM) Quanta FEG 250 (FEI) equipped with ET secondary electron detector and the beam accelerating voltage was 10 kV. Fourier Transform – Infrared spectra of the electrodes were registered using a spectrometer Nicolet iS50 FT-IR equipped with single-reflection diamond attenuated total reflectance (ATR) accessory ATR Special Quest. Spectra were recorded within the wavenumber range of 4000 - 400 cm^{-1}. Analysis of spectral data was performed using OMNIC software.

Electrochemical measurements

All voltammetric and impedance measurements were performed using BioLogic SP-150 potentiostat-galvanostat in a standard three-electrode configuration at room temperature. Ag | AgCl | 0.1M KCl was used as a reference electrode and platinum mesh as a counter electrode, respectively. The geometric surface area of the working electrode was 5×5 mm^2.

General characterization of the electrode / electrolyte interface for different types of membranes involved Cyclic Voltammetry in 1 M KCl solution containing 10 mM $Fe(CN)_6^{3-}$ / $Fe(CN)_6^{4-}$ redox pair. Calibration curve was performed in 0.1 X PBS with different amounts of glucose. Interference was evaluated also in 0.1 X PBS containing 5 mM of glucose and 0.1 mM of several compounds such as glycine (Gly), glutamine acid (GA), arginine (Arg), lactic acid, acetaminophen, acetylsalicylic acid and urea. During testing of the material integrity, the electrodes were measured in 0.1 X PBS with 5 mM of glucose. Long term stability was performed in 0.1 X PBS solution containing 5 mM glucose and 2% vol

of human serum. The electrode was measured for 7 days, one measurement each day. Between measurements the electrode was continuously kept in the diluted human serum solution to verify the effect of biofouling on the amperometric response. All electrolytes were air-saturated at room temperature and scan rate equaled to 50 mV/s.

Preliminary testing of the integrity of the electrode was tested by bending the plate with hands and after 20 bending cycles the CV curve is reported. The aim of this test is to provide environmental testing reflecting the natural utilization of the non-enzymatic sensing electrode.

Potentiostatic Electrochemical Impedance Spectroscopy experiments were carried out in two ways. First of them was general characterization in the presence of 10 mM ferrocyanide redox pairs in 1 M KCl air saturated electrolyte. In this case, before the recording of the impedance spectra, the electrodes were conditioned for 5 minutes at the formal potential of a redox pair (c.a. +0.22 V vs. Ag | AgCl | 0.1 K MCl). In the second case, the electrodes were measured in 0.1 X PBS without ferrocyanide before and after exposure to human serum. The purpose of this measurement was to verify the influence of biofouling on the electrochemical properties of the material. The applied potential was +0.30 V vs. Ag | AgCl | 0.1 M KCl to match the Au (0) to Au (I) oxidation peak.

The frequency ranges were set to be 10 kHz – 100 mHz and the amplitude of sinusoidal perturbative potential was 10 mV. The impedance data was fit through a complex nonlinear least squares (CNLS) procedure to the equivalent circuit using Powell algorithm embedded in EIS Spectrum Analyser software [29].

Results and discussion

Morphology of the electroactive substrate

A scheme of experimental setup for laser dewetting is depicted in Fig. 2a. Non-coated electrode after laser dewetting consists of quasi-periodic arrays of gold nanoparticles of 74 ± 10 nm diameter embedded in titanium nanodimples. SEM inspection confirming this structure is presented in Fig. 2b. The prepared heterostructure material exhibits good stability in alkaline and neutral media, particularly in the ones containing chlorides, as was shown in our previous papers [26,27] also containing detailed experimental data about both the dimpled titanium structure and properties of gold nanoparticles. Moreover, it possesses integrity and retains electrochemical activity towards glucose after numerous hand bending performed as a preliminary test. Detailed characterization of electrode materials can be found in [27,30].

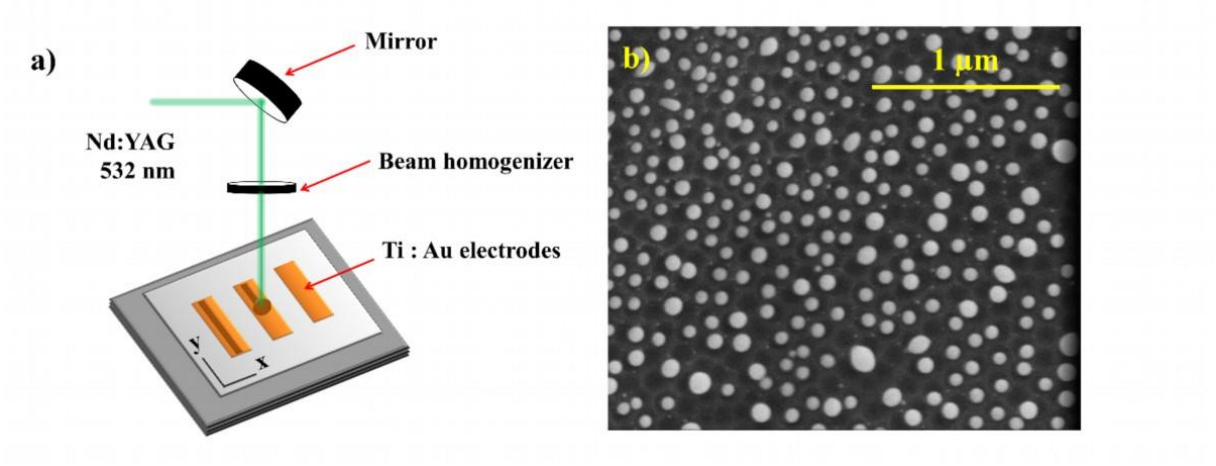

Fig. 2 a) Laser dewetting experimental setup, b). SEM inspection of TiND | AuNP electrode's morphology.

Characterization of electrodes covered with crosslinked poly(zwitterionic) coatings

After the photopolymerization of the pure zwitterionic mixture according to the procedure described in the experimental section, the electrode surface was coated with cured poly(zwitterion). The chemical structure of the coating is presented in Fig. 3 and it can be seen that the pSBMA chains are interconnected with EGDMA bridges.

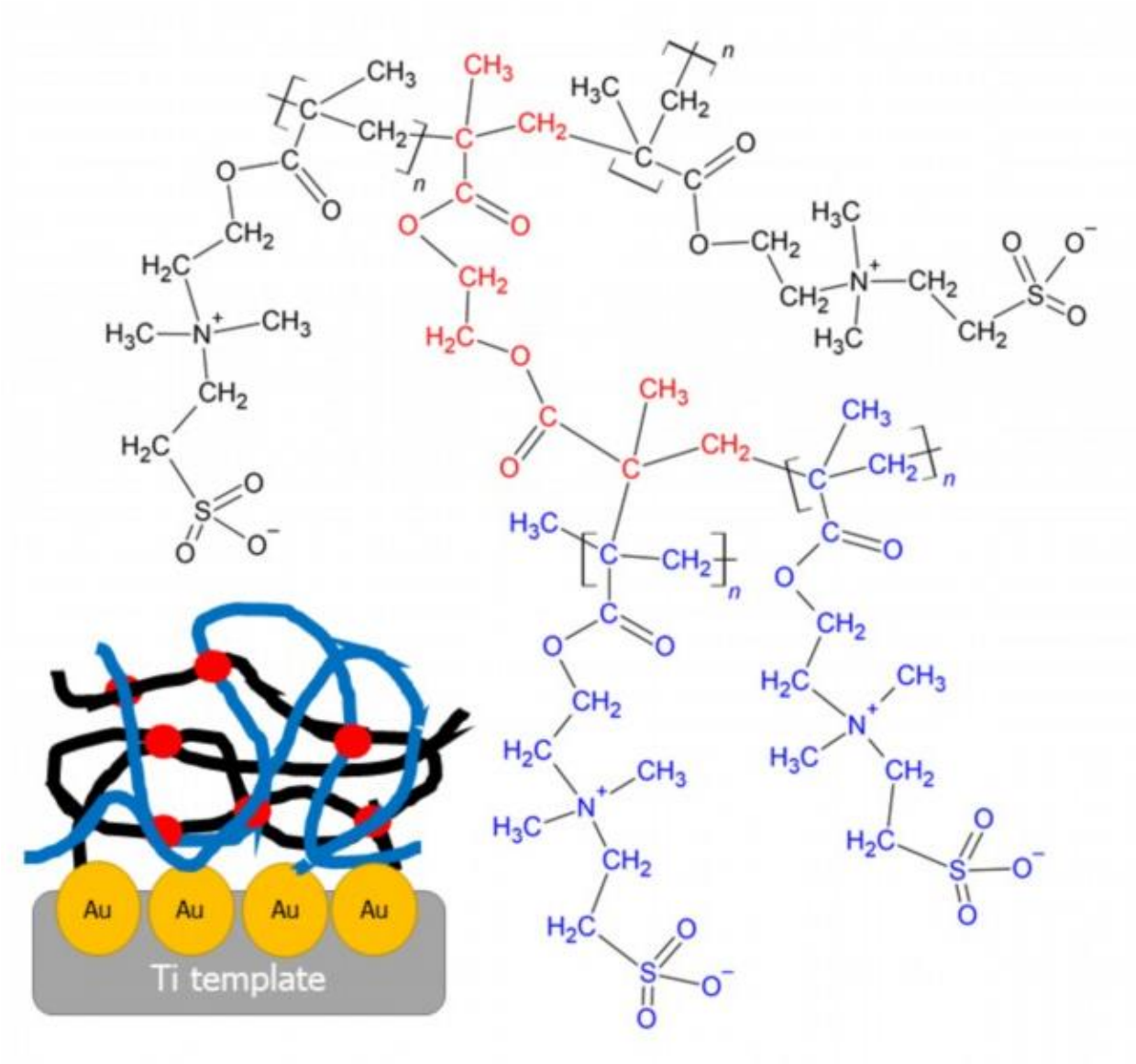

Fig. 3 Graphical representation of the modified electrode along with the chemical structure of the crosslinked poly(zwitterion).

The proposed structure is confirmed by FT-IR spectra given in Fig. 4a. There are a few characteristic absorption bands easily observed on the spectra for all three concentrations of the crosslinker. One can see broad medium bands between 3200 – 3700 cm^{-1} corresponding to O-H stretching vibrations of water absorbed into the pores and possibly traces of the photoinitiator [31]. There is one small band centered at 3000 cm^{-1} which can be attributed to C-H stretching bands from methylene group [32]. Another band at 1720 cm^{-1} is an evident C=O stretching vibration that comes from methacrylate carbonyls [32]. Low intensity band at 1650 cm^{-1} should correspond to C=C stretching modes of unreacted monomers. Another small band at 1480 cm^{-1} is likely to come from O-H deformation or C-N stretching vibrations. It is also non-negotiable that a large narrow band at 1160 cm^{-1} corresponds to S-O stretching and at 1030 cm^{-1} to C-O stretching modes [32]. The most probable origin of a variety of small bands in the range of 720 – 960 cm^{-1} is different modes of C-H groups such as bending, scissoring, and possibly C-S stretching

[33]. One can see a major difference between the coating with the highest crosslinking density (1:10) and the two others. It is the height of the band centered at 3500 cm^{-1} that is a few times lower compared to two other coatings with lower crosslinking densities. This suggests that the water content in the pores of this polymer is also the smallest.

Synthesized coatings maintain superior adhesion towards TiND | AuNP surface and for optimized UV exposure time (i.e. 3-10 minutes) no delamination or cracking occurs [34]. Although electrodes coated with pure poly(zwitterions) still exhibit catalytic activity towards glucose oxidation and are stable during bending cycles in the preliminary test, they lack the long-term stability in 0.1 X PBS solution because of swelling [35,36]. Moreover, the repeatability of fabrication process, measured as the current response towards glucose oxidation, was relatively low (Fig. 4b). Therefore, we decided to synthesize hybrid coatings consisting of both Nafion and PZ. It turned out that the only crosslinking ratio that allowed to obtain stable coatings was equal to 1:10 (EGDMA:SBMA). The improvement of repeatability can be seen in Fig. 4b and data used for this plot is provided in Fig. S1 in the Supporting Information file. Reduced tendency to swelling can be attributed to the fact that Nafion is prone to slight shrinking [37] in saline solutions while PZ to swelling. By combining the opposite properties of the two polymers, a higher level of stability was achieved. Moreover, it could be stated that Nafion strengthens the structure of PZ. A similar effect was observed for composite poly(zwitterionic) hydrogels with other polymers [38].

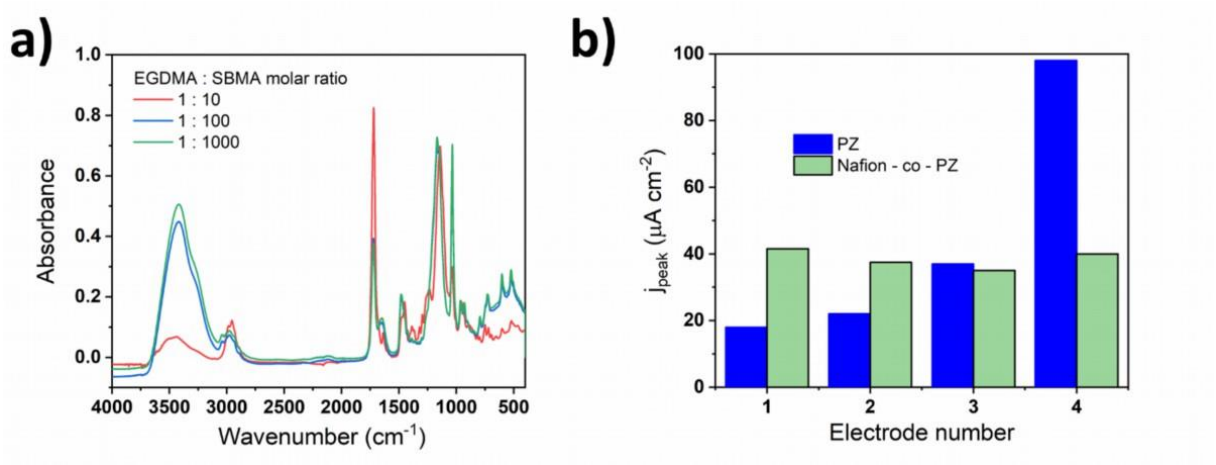

Fig. 4a) FT-IR spectra of electrodes coated with crosslinked poly(zwitterions) of different crosslinking density, b) comparison of repeatability of pure PZ and hybrid Nafion – co – PZ coating.

Characterization of electrodes covered with hybrid coatings

Three different experimental configurations of hybrid coatings were used to cover the electroactive materials. Detailed deposition procedure for each one is described in the Experimental section. The first of them was drop casting of Nafion and then photopolymerization of PZ. Electrodes covered with those coatings had strongly decreased activity towards glucose oxidation, possibly resulting from hampering of diffusion (Fig. S2). Moreover, there was a strong tendency towards swelling seen by naked eye for coatings with large PZ content. The second type of hybrid coating consisted of photopolymerized PZ with further drop-casted Nafion. In this scenario, catalytic activity was not diminished, although delamination was strongly pronounced, especially for large Nafion contents (Fig. S3). On the other hand, the third and the most stable configuration, namely, Nafion – co – PZ was introduced, where both photopolymerization and evaporation of Nafion solvent occurs simultaneously. Those coatings exhibited the broadest window of stability with only a slight decrease of catalytic activity after coating (Fig. S4). Therefore, this synthesis route was chosen for further studies towards glucose sensing. The optimum ratio of Nafion to PZ in this mixture was equal to 1:20. The ranges, where coatings preserve a sufficient integrity for three different coverages are schematically depicted in Fig. 5 and raw data obtained for the purpose of this scheme is provided in Fig.S2-S4. Additionally, the stability of electrodes after hand bending was maintained only when crosslink density was equal to 1:10. If the polymers were crosslinked in less degree (Fig. S5) swelling occurred more strongly.

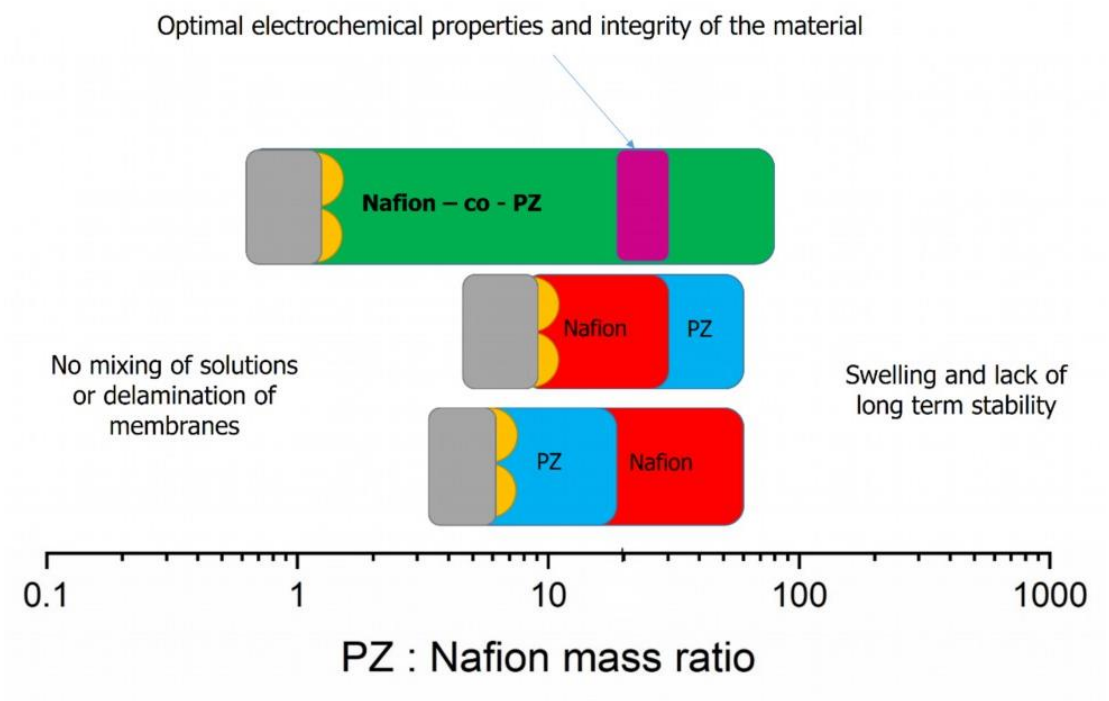

Fig. 5 Ranges of the integrity of the material for different hybrid coating configurations with respect to mass ratio of polymers.

Qualitative comparison of the chemical structures of Nafion – co – PZ with its pure polymer counterparts can be done by analyzing of FT-IR spectra in Fig. 6a. One can see that the structure of hybrid coating is very similar to the structure of pure PZ, which is anticipated. However there are a few distinguishable changes. The intensity of the wide O-H stretching band is slightly increased suggesting higher water content. C-H stretching band at 3000 cm^{-1} is decreased in the hybrid coating, because in the structure of Nafion there are no C-H bonds. There are also a few more small bands in the fingerprint region that are most probably attributed to C-F stretching modes of Nafion.

Cyclic voltammetry of electrodes coated with different polymers in the presence of ferrocyanide redox pairs is presented in Fig. 6b. One can see the quasi-reversible couple of oxidation and reduction peaks for all coatings, however there are a few distinctions between them. Peak potentials and peak to peak separation values are given in Tab. 2. First of all, pure PZ exhibits the lowest degree of symmetry, i.e., the oxidation current is higher than reduction current and the peaks are broadened with respect to other coatings. The possible explanation is that in this case the electron transfer process between ferrocyanides is more complex due to e.g. higher steric hindrance caused by polymer chains causing high charge transfer resistance [39,40,41]. Curves for electrodes coated with Nafion – co – PZ are rather similar to the one registered for the non-coated electrode, suggesting that charge transfer is only slightly hampered by the polymer.

EIS spectra presented in Fig. 6c also show tremendous differences between pure PZ and other coatings. In this case semicircle is significantly larger and both the real and imaginary parts of impedance are larger for all frequencies. Only this qualitative description suggests that for pure PZ coating oxidation is facilitated and reduction is hampered [41]. On the other hand, the remaining coatings maintain very small semicircles and therefore lower charge transfer resistance. In the low frequency region, a straight line almost 45 degrees sloping is present indicating Warburg diffusion behavior. Equivalent circuit (Fig. 6d) used for the fitting procedure consisted of solution resistance (R_s), constant phase element (CPE), charge transfer resistance (R_{ct}) and Warburg semi-infinite linear diffusion impedance (W) [42]. CPE element is necessary to be introduced because of inhomogeneous nature of double layer for the nanostructured electrode. Impedance of CPE is given by the formula [42]:

$$Z = \frac{1}{Q_0(j\omega)^n}$$

where Q_0 is related to the double layer capacitance, ω is an angular frequency of potential stimulus, j is an imaginary unit, and n is dimensionless parameter describing deviation from the pure capacitance behavior. Q_0 values can be used to calculate direct values of double layer capacitances according to the formula of Brug [43]:

$$\overline{C_{dl}} = {Q_0}^{1/n}\left[\frac{1}{R_s} + \frac{1}{R_{ct}}\right]^{1/(1-n)}$$

where C_{dl} is an average double layer capacitance. The values of equivalent circuit parameters obtained via non-linear least square procedure are given in Tab. 1. One can see that the electrolyte resistances are small and similar for all experiments. Charge transfer resistance fits the same range for all electrodes except the one coated with pure PZ. In this case, it is one order of magnitude higher, which indicates more sluggish charge transfer kinetics. It also corresponds very well with the result obtained by CV, i.e., lower current density. Double layer capacitance for the bare electrode and electrode covered with pure Nafion is similar, but in the case of hybrid coating it is 5 times greater. Such phenomenon might be attributed to the increased electric permittivity near the electrode compared to other electrodes. In zwitterionic media containing salts, the dielectric constant is locally deviated [44] and it depends on the conformation of the chains [45]. In other words, the microenvironment of the solution inside the polymer and the tendency to swelling seen by naked eye strictly correlate with the changes of dielectric constant and therefore double layer capacitance. Considering low values of n parameters, resulting C_{dl} data can be quantitative and incorrect [46,47], although it still can provide qualitative information.

Despite the fact that Nafion is present in only 5 wt. % and is responsible mainly for the enhancement of the stability and repeatability, the electrochemical quantities of hybrid coating obtained by EIS analysis are similar to pure Nafion. Following the abovementioned observations, one can state that hybrid Nafion – co – PZ coating exhibits the chemical structure of pure PZ but the electrochemical properties of Nafion.

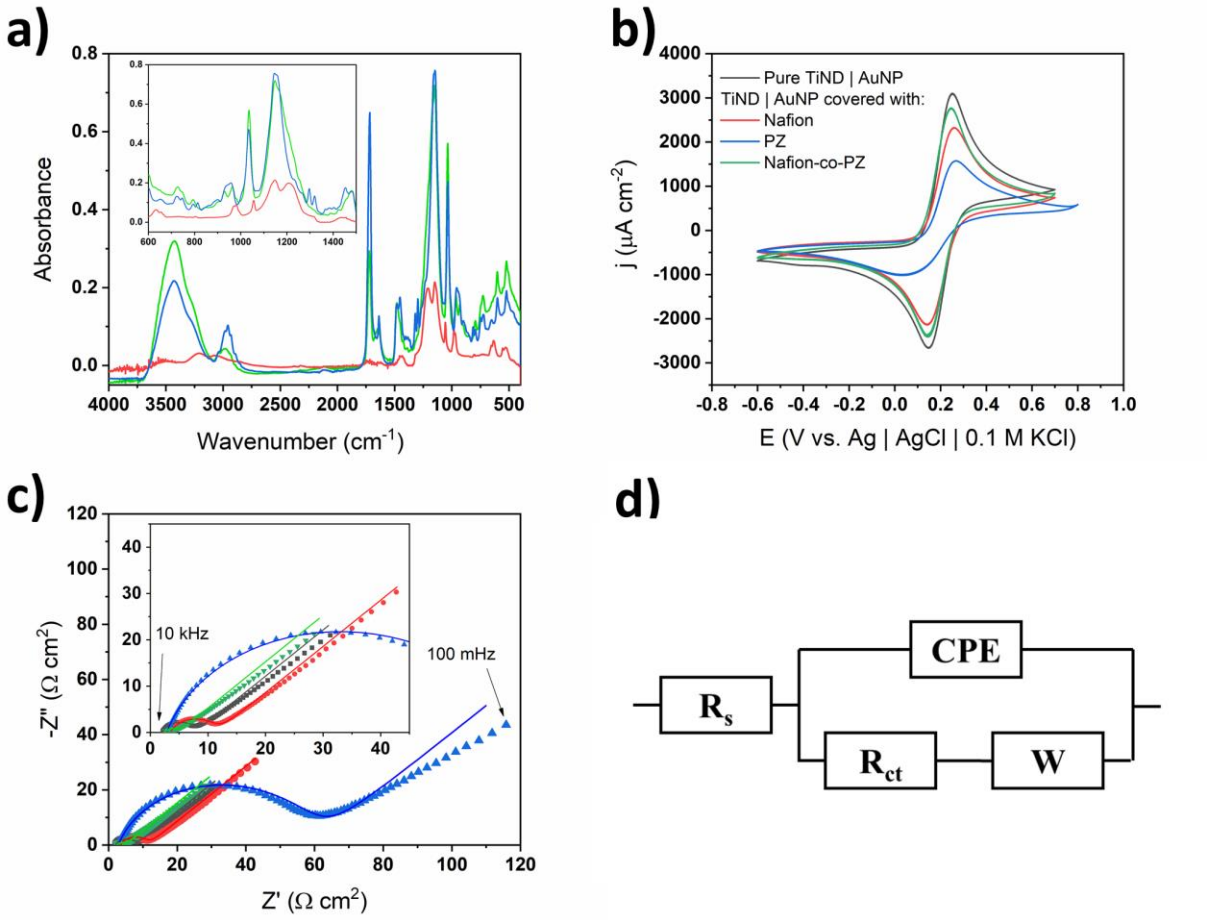

Fig. 6a) FT-IR spectra of pSBMA crosslinked coating with different molar ratio of compounds, b) CV curves, c) EIS spectra of different types of coatings (dotted lines indicate experimental data and solid lines fitter data), d) equivalent circuit used for fitting.

Tab. 1 The values of equivalent circuit parameters obtained from fitting of EIS spectra given in Fig. 6c (relative errors are given in parentheses).

	No membrane	Nafion	PZ	Nafion – co – PZ
R_s [Ω cm^2]	2.2 (1.5%)	3.5 (1.0%)	2.8 (1.8%)	2.4 (1.7%)
R_{ct}[Ω cm^2]	5.9 (1.6%)	8.1 (1.1%)	57.4 (1.4%)	3.0 (3.5%)
Aw [Ω cm^2 s$^{-1/2}$]	18.3 (1.8%)	24.9 (1.3%)	39.8 (3.8%)	29.5 (2.1%)
Q_0 [µF cm^{-2} s^{n-1}]	139 (3.0%)	111 (2.3%)	62.5 (1.7%)	320 (14.9%)
n	0.78 (0.4 %)	0.76	0.81 (0.2%)	0.73 (1.1%)
C_{dl} [mF cm^{-2}]	0.63	0.65	0.21	3.00
$\chi^2 \times 10^{-4}$	8.2	3.9	11	24

Tab. 2 Peak potentials and peak to peak separation data of CV curves presented on Fig. 6b

Electrode	Oxidation peak potential [mV]	Reduction peak potential [mV]	Peak to peak separation [mV]
Pure TiND | AuNP	255	149	106
Nafion	262	142	120
PZ	268	40	228
Nafion – co - PZ	245	146	99

Glucose sensing properties of electrodes coated with hybrid poly(zwitterions)

Fig. 7a shows a series of cyclic voltammograms registered in 0.1 X PBS for TiND | AuNP electrode coated with hybrid Nafion – co – PZ. One can see that during the forward scan there are two oxidation peaks consistently growing with the increasing glucose concentration. The first of them is located at +0.25 V and corresponds to the creation of Au(I) layer and subsequent catalytic oxidation of glucose to gluconolactone. The second lies at +0.7 V (shifting to +1.0 V for higher glucose concentrations) and can be attributed to the oxidation of Au(I) to Au(III) species. In this region there is another process involving direct oxidation of glucose to Au(III) species that can also occur [2,11]. Two reduction peaks are also present on the reverse scan at voltammograms. The first of them at +0.25 V corresponds to the reduction of Au(III) to Au(I) species and second is attributed to both Au(I) to Au(0) reduction as well as the reduction of the passivated titanium dioxide layer, i.e. Ti(IV) to Ti(III). Inset shows the calibration curve for different glucose concentrations in the range of 0-12 mM. Current increase is linear in the range from 0.1 mM to 2 mM with sensitivity equal to 11 $\mu A\ cm^{-2}\ mM^{-1}$ and in the second range with a sensitivity of 3 $\mu A\ cm^{-2}\ mM^{-1}$. The presence of an inflection point at 2 mM might be connected with the change of dominant oxidation mechanism discussed profoundly in our previous work [48]. However, in the logarithmic scale the linear range is significantly wider, i.e. 0.4 mM – 12 mM with sensitivity equal to 36.8 $\mu A\ cm^{-2} mM^{-1}$ (Fig. S6). This range is sufficient to cover concentration ranges in most physiological fluids [14]. The limit of detection equals to 23 μM. A comparison of sensing parameters with other materials is presented in Tab. 3. Differences between sensitivity and limit of detection between electrodes modified with pure PZ (Fig. S7) and Nafion – co – PZ are not significant, whereas linear range is widened in case of hybrid membranes. One can see that limit of detections for TiND | AuNP structures is among the lowest indicating the high catalytic activity in lower glucose concentrations. It is worth remembering that our studies are performed in 0.1 X PBS containing at least

13 mM of chloride with pH=7.4, not in 0.1 M NaOH where the formation of hydroxide is much more facilitated due to larger amount of adsorbed electrocatalytic $AuOH_{ads}$ species [48].

Fig.7b shows the glucose oxidation current density in 0.1 X PBS containing 5 mM of glucose upon increasing the number of bending cycles in the preliminary testing. One can see that even after 1000 bends current density stays roughly the same, indicating that Nafion-co-PZ maintains integrity and therefore the response is considered stable. This was the highest number of bendings achieved among of Nafion, PZ and Nafion – co – PZ membranes. Raw CV data used for making this plot was provided in Fig. S8.

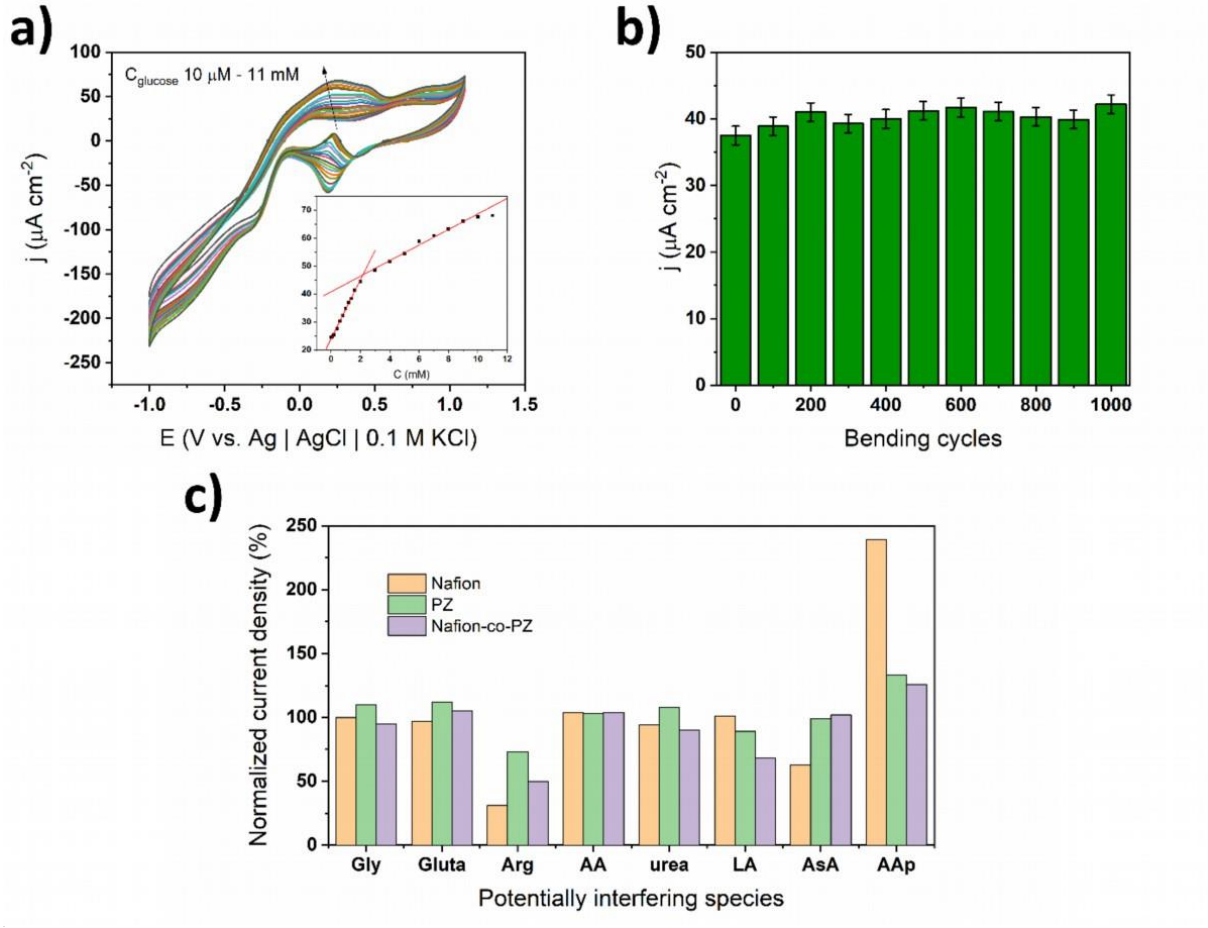

Fig. 7a) Cyclic voltammograms of gold-based electrode covered with hybrid Nafion – co – PZ coating registered in 0.1 X PBS with different glucose concentrations; inset is the calibration curve, b) electrochemical response of electrode material in 0.1 X PBS containing 5 mM glucose after different amount of bending cycles in the preliminary test, c) interference of different compounds in 0.1 X PBS containing 5 mM glucose. Current densities for different membranes were normalized to 100% with respect to each background current without interferants.

Interference tests for all three types of polymer films are gathered in Fig. 7c. Considering different background currents (at +0.3 V) for those coatings, all currents were normalized so that the response

towards pure 5 mM glucose is set to 100% and all other currents are rescaled with respect to that value (raw data is presented in Fig. S9). The closer the current is to 100% line, the less interference is observed. One can see that for glycine, GA, AA, and urea all coatings preserve roughly the same current response, meaning there is only a small interference effect. However, in the case of the electrode with pure Nafion, the presence of AsA leads to reduction and the presence of AAp leads to the increase of oxidation current. However, the introduction of PZ or Nafion-co-PZ allows to increase or decrease the current responses, correspondingly. Straightforwardly, it implies that the zwitterionic nature of PZ chains allows to reduce the interference from those two analgesics.

Tab. 3 Comparison of glucose sensing parameters for different electrodes measured at pH = 7.4.

Electrode type	Technique	Sensitivity [μA cm^{-2} mM^{-1}]	LOD [μM]	Linear range [mM]	Reference
TiND | AuNP | PZ	**CV**	**15.4**	**13**	**0.2 – 1.0**	**Current work (Fig. S7)**
TiND | AuNP | Nafion – co – PZ	**CV**	**11**	**23**	**0.1 – 2.0 (linear)**	**Current work (Fig. 7a)**
		36.8	**-**	**0.4 – 12.0 (logarithmic)**	
FcBA/glucose/ /3APBA/4MBA/ /AuNPs/ITO	CV/DPV	0.56	43	0.5 – 30	[49]
FcBA/glucose/ /3APBA/SPCE	DPV	5.8	100	0.5 – 20	[50]
PBA/PMS/GCE	CV/DPV	2.64	7.8	0.02 – 0.5	[51]
Spike like Au microelectrode	CV	1.7	48	0.1 – 0.5	[52]
		2.4	-	1 – 30	
AuNPs | Chitosan | GCE	CV	66	100	0.2 – 110	[53]

Lastly, electrode's efficiency was tested in human serum diluted (2% vol.) with 0.1 X PBS. Cyclic voltammograms were registered each day during the 7 days period of electrode's exposure (Fig. 8a).

Oxidation current density was keeping stable for 4 days then the signal was starting to decrease (raw data presented in Fig. S10). This change was attributed to biofouling due to pH drop of the solution. pH was staying stable during four days (between 7.46 to 7.38), but at the end of the experiment, i.e. after 7 days it dropped to 6.34. Possible reason of pH drop is absorption of CO_2 by electrolyte. This hypothesis has been verified in a following way. Another similar electrode was measured daily during 10 days. However the serum sample was being changed every day so that pH had been kept constant and equal to 7.4. Electrode was kept under vacuum in desiccator so that no CO_2 could be absorbed during storage. In this scenario activity of the material was not lost and current density maintained stable during 10 day period. Therefore one can suggest that the decrease of pH leads to the protonation of sulfonate groups of sulfobetaine methacrylate chains in Nafion – to – PZ membrane. The result is that the zwitterionic character of the coating is lost. As a consequence, an adsorbed layer of some organic compounds was created, which can be seen on FT-IR spectra in Fig. 8c. Some bands after exposure are distorted especially at 3400, 3000, 1700, and 1550 cm^{-1}. CVs performed at the end of the shelf live test (7^{th} day) also suggest decreased electroactive surface area, because all redox peaks were reduced, not only the one connected with glucose oxidation. Moreover, one can observe the changes of EIS spectra recorded in 0.1 X PBS before and after exposure to human serum (Fig. 8d and Tab. 4). In particular, the double layer capacitance decreased after exposure, which is in agreement with the hypothesis of reduced active surface area. Additionally, Warburg element corresponding to diffusion towards the electrode was two times increased. This value is inversely proportional to the diffusion coefficient [42] near the electrode, meaning it has grown up during the exposure in serum. That is another argument supporting the statement regarding biofilm formation. Although considering both FT-IR and EIS spectra, there are no evidence for the pore closing processes. This phenomenon was observed in the case of pure Nafion membranes and thoroughly described in our previous paper [14].

Photopolymerized zwitterions can be used as a versatile coating for non-enzymatic glucose sensors with improved antifouling properties and easy fabrication route. Several perspectives for further research emerge Future plans for the work involve improvements in the fabrication procedure to enable industrial production of electrodes as well as the construction of the device working on a real subjects.

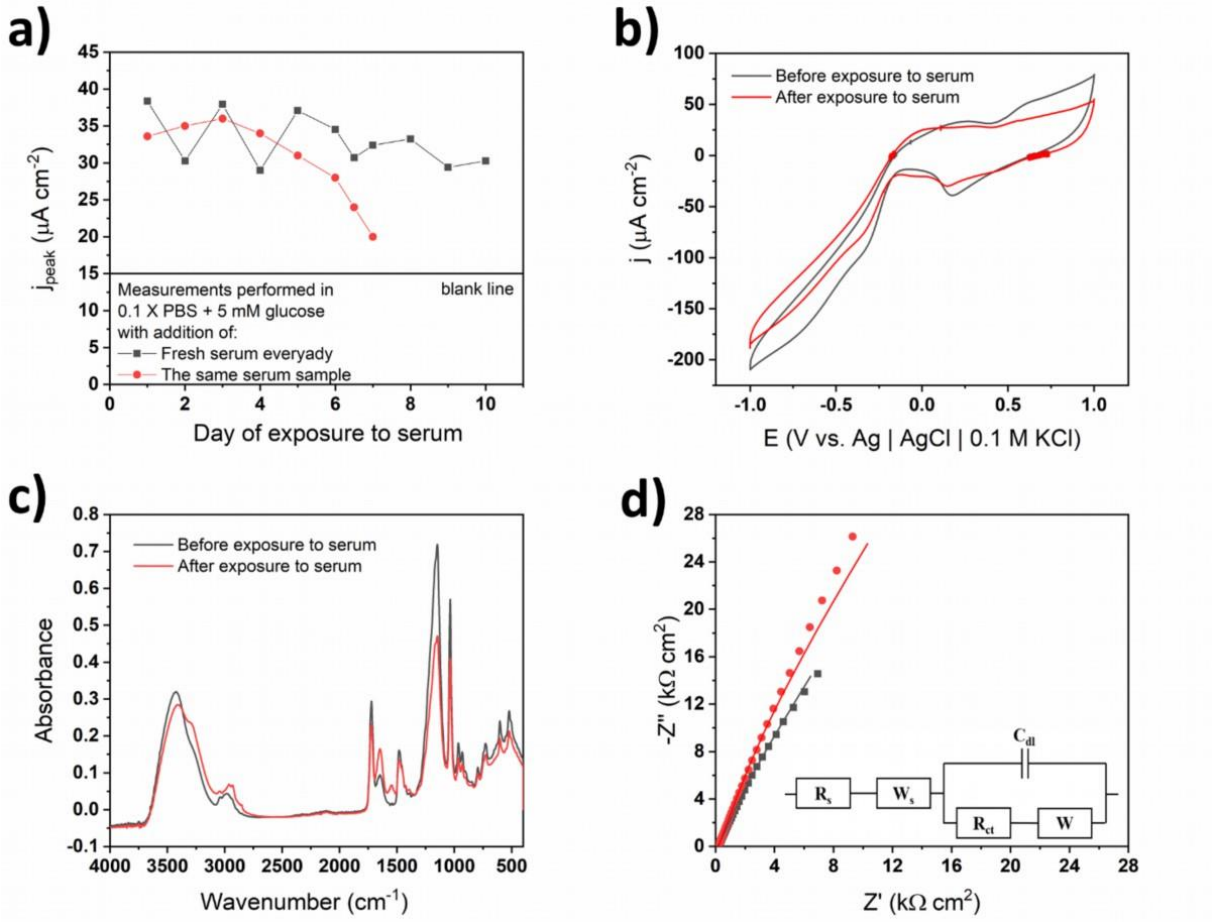

Fig. 8 a) Oxidation current density changes of electrodes coated with Nafion – co – PZ during exposure to diluted human serum, b) CV curves in diluted human serum at the first and last day of exposure, c) FT-IR spectra of coated electrode before and after exposure to diluted human serum, d) EIS spectra registered in 0.1 X PBS (dotted lines indicate experimental data and solid lines fitter data)

Tab. 4 Equivalent circuit parameters obtained from fitting of EIS data from Fig. 8d (relative errors are given in parentheses).

	Before exposure	After exposure
R_s [kΩ cm^2]	0.12 (0.7%)	0.15 (1.0%)
R_{ct} [kΩ cm^2]	3.90 (0.4%)	3.58 (0.7%)
Aw [kΩ s$^{-1/2}$]	9.56 (6.0%)	21.70 (7.9%)
C [μF/cm^2]	71.7 (2.3%)	37.8 (2.9%)
Aw_s [kΩ s$^{-1/2}$]	1.47 (0.8%)	1.72 (1.4%)
B	0.84 (3.2%)	0.83 (6.4%)

$\chi^2 \times 10^{-5}$	9.6	22.0

Conclusions

Poly(zwitterionic) coatings were deposited onto electroactive materials based on gold nanoparticles on titanium substrate via the optimized photopolymerization approach. PZ exhibits superior adhesion towards Au-Ti surface that is of high importance for further sensing purposes. When PZ are strongly crosslinked with a molar ratio of 1: 10, the water content is the smallest. Compositions created with this ratio also exhibit better integrity when compared to Nafion. Nafion – co – PZ hybrids are more repeatable than pure PZ and possess enhanced long – term stability than pure PZ ones. The highest electrochemical activity with sustained integrity represented PZ : Nafion mixture with mass ratio equal to 20:1. Despite this large excess of PZ, EIS and CVs suggest that the surface properties of the hybrid coating are more similar to Nafion's surface instead of pure PZ. Despite the presence of insulating membrane, sensing properties such as 36.8 μA cm^{-2} mM^{-1} and 23 μM limit of detection remain similar to the bare electrode. Materials covered with the hybrid membrane retain the electrochemical response even after 1000 bends. There is a synergistic effect of the two polymers that causes reduction of AsA and AAp interference as well as enhanced stability in diluted human serum. After 4 days of exposure to serum, electrochemical signal started to decrease because of pH drop and therefore protonation of sulfonate groups.

Credit Author statement

Adrian Olejnik: Conceptualization, Investigation, Formal analysis, Visualization, Writing - Original Draft

Jakub Karczewski: Investigation

Anna Dołęga: Investigation

Katarzyna Siuzdak: Conceptualization, Validation, Visualization, Writing - Original Draft, Writing - Review & Editing, Resources

Adam Cenian: Methodology, Writing - Review & Editing

Katarzyna Grochowska: Conceptualization, Validation, Writing - Original Draft, Writing - Review & Editing, Supervision, Resources, Funding acquisition

References

[1] Chakraborty, P., Dhar, S., Debnath, K., Majumder, T., & Mondal, S. P. (2019). Non-enzymatic and non-invasive glucose detection using Au nanoparticle decorated CuO nanorods. *Sensors and Actuators B: Chemical*, *283*, 776-785.

[2] Hwang, D. W., Lee, S., Seo, M., & Chung, T. D. (2018). Recent advances in electrochemical non-enzymatic glucose sensors–a review. *Analytica chimica acta*, *1033*, 1-34.

[3] Park, S., Park, S., Jeong, R.-A., Boo, H., Park, J., Kim, H. C., & Chung, T. D. (2012). Nonenzymatic continuous glucose monitoring in human whole blood using electrified nanoporous Pt. Biosensors and Bioelectronics, 31(1), 284–291.

[4] Strakosas, X., Selberg, J., Pansodtee, P., Yonas, N., Manapongpun, P., Teodorescu, M., & Rolandi, M. (2019). A non-enzymatic glucose sensor enabled by bioelectronic pH control. *Scientific reports*, *9*(1), 1-7.

[5] Ernst, S., Heitbaum, J., & Hamann, C. H. (1979). The electrooxidation of glucose in phosphate buffer solutions: Part I. Reactivity and kinetics below 350 mV/RHE. *Journal of Electroanalytical Chemistry and Interfacial Electrochemistry*, *100*(1-2), 173-183.

[6] Hsiao, M. W., Adžić, R. R., & Yeager, E. B. (1996). Electrochemical oxidation of glucose on single crystal and polycrystalline gold surfaces in phosphate buffer. *Journal of the Electrochemical Society*, *143*(3), 759.

[7] Becerik, I., & Kadirgan, F. (1992). The electrocatalytic properties of palladium electrodes for the oxidation of d-glucose in alkaline medium. *Electrochimica acta*, *37*(14), 2651-2657.

[8] Berchmans, S., Gomathi, H., & Rao, G. P. (1995). Electrooxidation of alcohols and sugars catalysed on a nickel oxide modified glassy carbon electrode. *Journal of Electroanalytical Chemistry*, *394*(1-2), 267-270.

[9] Marioli, J. M., & Kuwana, T. (1992). Electrochemical characterization of carbohydrate oxidation at copper electrodes. *Electrochimica Acta*, *37*(7), 1187-1197.

[10] Cataldi, T. R., Guerrieri, A., Casella, I. G., & Desimoni, E. (1995). Study of a cobalt-based surface modified glassy carbon electrode: Electrocatalytic oxidation of sugars and alditols. *Electroanalysis*, *7*(4), 305-311.

[11] Toghill, K. E., & Compton, R. G. (2010). Electrochemical non-enzymatic glucose sensors: a perspective and an evaluation. *Int. J. Electrochem. Sci*, *5*(9), 1246-1301.

[12] Moatti-Sirat, D., Velho, G., & Reach, G. (1992). Evaluating in vitro and in vivo the interference of ascorbate and acetaminophen on glucose detection by a needle-type glucose sensor. *Biosensors and Bioelectronics*, *7*(5), 345-352.

[13] Yang, X., Pan, X., Blyth, J., & Lowe, C. R. (2008). Towards the real-time monitoring of glucose in tear fluid: Holographic glucose sensors with reduced interference from lactate and pH. *Biosensors and Bioelectronics*, *23*(6), 899-905.

[14] Olejnik, A., Karczewski, J., Dołęga, A., Siuzdak, K., & Grochowska, K. (2020). Novel approach to interference analysis of glucose sensing materials coated with Nafion. *Bioelectrochemistry*, 107575.

[15] Gooding, J. J. (2019). Finally, a simple solution to biofouling. *Nature nanotechnology*, *14*(12), 1089-1090.

[16] Schlenoff, J. B. (2014). Zwitteration: coating surfaces with zwitterionic functionality to reduce nonspecific adsorption. *Langmuir*, *30*(32), 9625-9636.

[17] Baggerman, J., Smulders, M. M., & Zuilhof, H. (2019). Romantic Surfaces: A Systematic overview of stable, biospecific, and antifouling zwitterionic surfaces. *Langmuir*, *35*(5), 1072-1084.

[18] Laschewsky, A., & Rosenhahn, A. (2018). Molecular design of zwitterionic polymer interfaces: searching for the difference. *Langmuir*, *35*(5), 1056-1071.

[19] Gorzolnik, B., Mela, P., & Moeller, M. (2006). Nano-structured micropatterns by combination of block copolymer self-assembly and UV photolithography. *Nanotechnology*, *17*(19), 5027.

[20] Ni, L., Chemtob, A., Croutxé-Barghorn, C., Moreau, N., Bouder, T., Chanfreau, S., & Pébère, N. (2014). Direct-to-metal UV-cured hybrid coating for the corrosion protection of aircraft aluminium alloy. *Corrosion science*, *89*, 242-249.

[21] Andrzejewska, E. (2020). Free-radical photopolymerization of multifunctional monomers. In *Three-Dimensional Microfabrication Using Two-Photon Polymerization* (pp. 77-99). William Andrew Publishing.

[22] Fouassier, J. P., & Rabek, J. F. (Eds.). (1993). *Radiation curing in polymer science and technology: Fundamentals and methods* (Vol. 1). Springer Science & Business Media.

[23] Kaur, M., & Srivastava, A. K. (2002). PHOTOPOLYMERIZATION: A REVIEW. Journal of Macromolecular Science, Part C: Polymer Reviews, 42(4), 481–512. doi:10.1081/mc-120015988

[24] Leigh, B. L., Cheng, E., Xu, L., Andresen, C., Hansen, M. R., & Guymon, C. A. (2017). Photopolymerizable Zwitterionic Polymer Patterns Control Cell Adhesion and Guide Neural Growth. Biomacromolecules, 18(8), 2389–2401.

[25] Yang, W., Xue, H., Carr, L. R., Wang, J., & Jiang, S. (2011). Zwitterionic poly(carboxybetaine) hydrogels for glucose biosensors in complex media. Biosensors and Bioelectronics, 26(5), 2454–2459.

[26] Olejnik, A., Siuzdak, K., Karczewski, J., & Grochowska, K. (2020). A Flexible Nafion Coated Enzyme-free Glucose Sensor Based on Au-dimpled Ti Structures. *Electroanalysis*, *32*(2), 323-332.

[27] Grochowska, K., Szkoda, M., Karczewski, J., Śliwiński, G., & Siuzdak, K. (2017). Ordered titanium templates functionalized by gold films for biosensing applications–Towards non-enzymatic glucose detection. *Talanta*, *166*, 207-214.

[28] Latif, U., Dickert, F. L., Blach, R., & Feucht, H. (2013). Biocompatible membranes and coatings for glucose sensor. *J. Chem. Soc. Pak*, *35*(1), 17.

[29] Bondarenko A. S., Ragoisha G. A. In Progress in Chemometrics Research, Pomerantsev A. L., Ed.; Nova Science Publishers: New York, 2005, pp. 89–102 (the program is available online at http://www.abc.chemistry.bsu.by/vi/analyser/)

[30] Grochowska, K., Siuzdak, K., Sokołowski, M., Karczewski, J., Szkoda, M., & Śliwiński, G. (2016). Properties of ordered titanium templates covered with Au thin films for SERS applications. *Applied Surface Science*, *388*, 716-722.

[31] https://webbook.nist.gov/cgi/cbook.cgi?ID=C582241&Type=IR-SPEC&Index=3

[32] Lalani, R., & Liu, L. (2011). Synthesis, characterization, and electrospinning of zwitterionic poly (sulfobetaine methacrylate). *Polymer*, *52*(23), 5344-5354.

[33] Crowder, G. A. (1972). The CS Stretching Frequency in Thiol Acids and Esters. *Applied Spectroscopy*, *26*(4), 486-487.

[34] Thouless, M. D. (1991). Cracking and delamination of coatings. *Journal of Vacuum Science & Technology A: Vacuum, Surfaces, and Films*, *9*(4), 2510-2515.

[35] A. Olejnik (2020). Wykorzystanie technologii laserowego przetapiania do wytwarzania elektrod z powłoką ochronną czułych względem glukozy, Gdansk University of Technology, Master Thesis

[36] Huglin, M. B., & Rego, J. M. (1991). Influence of temperature on swelling and mechanical properties of a sulphobetaine hydrogel. *Polymer*, *32*(18), 3354-3358.

[37] Tang, H., Peikang, S., Wang, F., & Pan, M. (2007). A degradation study of Nafion proton exchange membrane of PEM fuel cells. *Journal of Power Sources*, *170*(1), 85-92.

[38] Shen, J., Du, M., Wu, Z., Song, Y., & Zheng, Q. (2019). Strategy to construct polyzwitterionic hydrogel coating with antifouling, drag-reducing and weak swelling performance. *RSC advances*, *9*(4), 2081-2091.

[39] Compton, R. G., & Banks, C. E. (2018). *Understanding voltammetry*. World Scientific.

[40] Bogdanowicz, R., Ficek, M., Malinowska, N., Gupta, S., Meek, R., Niedziałkowski, P., Rycewicz, M., Sawczak, M., Ryl, J. &Ossowski, T. (2020). Electrochemical performance of thin free-standing boron-doped diamond nanosheet electrodes. Journal of Electroanalytical Chemistry, 114016.

[41] Winkler, K. (1995). The kinetics of electron transfer in Fe (CN) 64− 3− redox system on platinum standard-size and ultramicroelectrodes. *Journal of Electroanalytical Chemistry*, *388*(1-2), 151-159.

[42] Lasia, Andrzej. (2014). A. Lasia, Electrochemical Impedance Spectroscopy and its Applications, book, Springer, 2014. 10.1007/978-1-4614-8933-7.

[43] Brug, G. J., Van Den Eeden, A. L. G., Sluyters-Rehbach, M., & Sluyters, J. H. (1984). The analysis of electrode impedances complicated by the presence of a constant phase element. *Journal of Electroanalytical Chemistry*, *176*(1-2), 275-295.

[44] Kumar, R., & Fredrickson, G. H. (2009). Theory of polyzwitterion conformations. *The Journal of Chemical Physics*, *131*(10), 104901.

[45] Azzaroni, O., Brown, A. A., & Huck, W. T. (2006). UCST wetting transitions of polyzwitterionic brushes driven by self-association. *Angewandte Chemie*, *118*(11), 1802-1806.

[47] Łosiewicz, B., Jurczakowski, R., & Lasia, A. (2017). Kinetics of hydrogen underpotential deposition at iridium in sulfuric and perchloric acids. *Electrochimica Acta*, *225*, 160-167.

[48] Olejnik, A., Karczewski, J., Dołęga, A., Siuzdak, K., & Grochowska, K. (2020). Insightful Analysis of Phenomena Arising at the Metal| Polymer Interphase of Au-Ti Based Non-Enzymatic Glucose Sensitive Electrodes Covered by Nafion. *Coatings*, *10*(9), 810.

[49] Chen, M., Cao, X., Chang, K., Xiang, H., & Wang, R. (2020). A Novel Electrochemical Non-enzymatic Glucose Sensor Based on Au Nanoparticle-Modified Indium Tin Oxide Electrode and Boronate Affinity. *Electrochimica Acta*, 137603.

[50] Li, J., Bai, Z., Mao, Y., Sun, Q., Ning, X., & Zheng, J. (2017). Disposable Sandwich-type Electrochemical Sensor for Selective Detection of Glucose Based on Boronate Affinity. Electroanalysis, 29(10), 2307–2315.

[51] Li, J., Liu, L., Wang, P., Yang, Y., & Zheng, J. (2014). Amplified detection of saccharide based on redox-poly(phenol-co-3-hydroxyphenylboronic acid) coupling with a redox cycling. Sensors and Actuators B: Chemical, 198, 219–224.

[52] Hovancová, J., Niščáková, V., Šišoláková, I., Oriňaková, R., Maskaľová, I., Oriňak, A., & Kovaľ, K. (2020). Gold Microelectrodes Decorated by Spike-Like Nanostructures as a Promising Non-Enzymatic Glucose Sensor. *Electroanalysis*.

[53] Karra, S., Wooten, M., Griffith, W., & Gorski, W. (2016). Morphology of gold nanoparticles and electrocatalysis of glucose oxidation. *Electrochimica acta*, *218*, 8-14.